

³Transitions corresponding to quantum absorption [$0 \leq |V| \leq |\Delta(\text{In}) + \Delta(\text{Al})|$] have not as yet been observed. As in the case of Pb, this is thought to reflect the low equilibrium excitation of the energy reservoir (at 1.1°K) to which tunneling electrons couple.

⁴Similar effects are observed in Pb although there

the situation is further complicated by the apparent multiple-gap behavior associated with thick Pb films.

⁵It is conceivable that such features may be related to the type of infrared-absorption structure observed for single crystals of Sn. P. L. Richards, Phys. Rev. Letters 7, 412 (1961).

de HAAS-van ALPHEN EFFECT, MAGNETIC BREAKDOWN, AND THE FERMI SURFACE OF CADMIUM*

D. C. Tsui† and R. W. Stark‡

Institute for the Study of Metals and Department of Physics, The University of Chicago, Chicago, Illinois
(Received 6 December 1965)

The accepted model for the Fermi surface of cadmium is the modified single-orthogonalized-plane-wave (OPW) surface first proposed by Harrison.¹ This surface must be described in the single-zone scheme since the degeneracy of the energy bands across the *AHL* symmetry plane of the hexagonal-close-packed Brillouin zone is removed when spin-orbit interaction effects are considered.² The results of a number of previous experiments³ pertinent to the electronic band structure of cadmium have been interpreted in terms of this model. Our de Haas-van Alphen (dHvA) and magnetoresistance investigations in cadmium indicate that this description of its Fermi surface is incorrect in certain essential details. The purpose of this Letter is to describe the model which fits our data (as well as data previously published) and, in addition, to discuss some interesting magnetic breakdown⁴ effects which we have observed.

The dHvA measurements were taken in magnetic field strengths extending to 38 kG utilizing low-frequency field-modulation techniques.⁵ The crystals used in these investigations were purified by zone refining and had residual resistance ratios ($R_{300^\circ\text{K}}/R_{1.1^\circ\text{K}}$) of 39 000. The extremal cross-sectional area branches which were derived from the observed dHvA frequencies⁶ and which are pertinent for this discussion are shown for the major crystallographic planes on a semilog plot in Fig. 1. The angular variation of each of these branches was determined from field-rotation diagrams.⁷ The data are accurate to 0.1%.

The extremal-area branches α and β_1 in Fig. 1 have been observed in previous experiments. However, they were thought to be degenerate along (0001) and hence consistent with a six-

fold set of cylinders whose major axes were tilted 28.5° from (0001) toward (11 $\bar{2}$ 0). These were assigned to diagonal arm modifications of the hole sheet in the second zone of the single OPW model.¹ Our measurements show that these two branches are not degenerate at (0001) and that in fact they arise on sheets of the Fermi surface which have an axis of symmetry along (0001). Branch α arises on a closed sheet of the Fermi surface. We have assigned it to the hole sheet in the first zone of the single-OPW

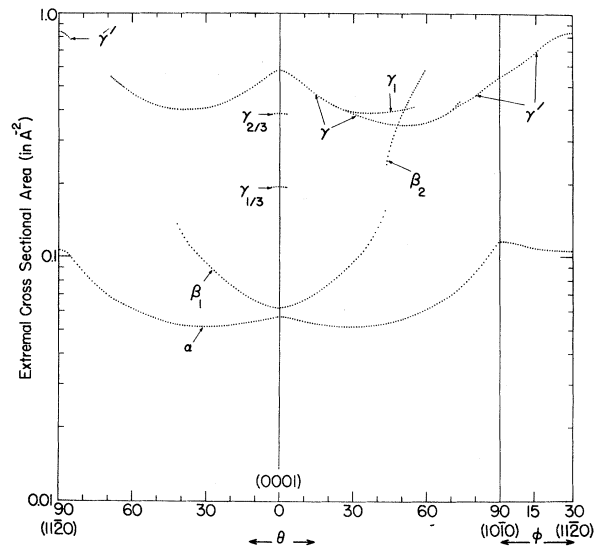


FIG. 1. The extremal dHvA cross-sectional area branches associated with the sheets of the Fermi surface in the first and second Brillouin zones of cadmium. The polar angle, θ , measures the angle between (0001) and the magnetic field direction. The azimuthal angle, ϕ , measures the angle between (10 $\bar{1}$ 0) and the direction of the magnetic field when the latter is in the basal plane. The unit of area is reciprocal square angstroms.

model (the "cap") shown in Fig. 2(a). This assignment is surprisingly consistent since both the size and variation with θ of the extremal cross-sectional area of the single-OPW "cap" follows that of α very closely even to the extent of having an absolute minimum in area at $\theta = 28.5^\circ$. The inflection point in α occurs within 2° of $(10\bar{1}0)$ in the $(11\bar{2}0)$ plane. Our analysis of the experimental data indicates that the cap is long and sharply peaked, extending nearly to K along the KH line of the Brillouin zone.

The assignment of β_1 results quite naturally from the identification of α . The first-zone "cap" is split off from the hole sheet in the second zone [an undulating cylinder shown in Fig. 2(b)] by a small energy gap ($\sim 5 \times 10^{-3}$ Ry) which arises as a result of the effect of spin-

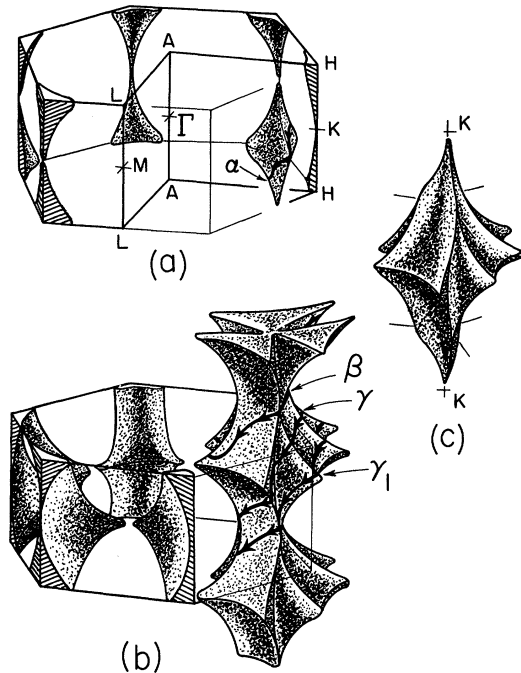


FIG. 2. The symmetry points of the hexagonal-close-packed Brillouin zone are shown in Fig. 2(a) together with the hole segments of the Fermi surface in the first zone. The segments are also shown remapped to form the "cap" with a typical extremal orbit associated with branch α in Fig. 1 drawn on its surface. Fig. 2(b) shows the second-zone hole sheet (an undulating cylinder) both as single-zone segments and in the extended-zone scheme. Typical extremal orbits associated with branches β , γ , and γ_1 in Fig. 1 are shown on the extended-zone-scheme surface. Fig. 2(c) shows the closed surface which results when magnetic breakdown causes the electrons to ignore the spin-orbit coupling-induced gap across the AHL plane of the zone. The undulating cylinder is terminated at the AHL plane and "capped" by the first zone segments.

orbit interactions. The perturbation reduces the area of intersection of the "cap" with the AHL plane of the zone and increases the area of intersection of the undulating cylinder. Hence, α and β_1 arise as a pair. β_1 results from the orbits around the junction of the second-zone undulating cylinder with the AHL plane. The β_1 is cut off quite sharply at $\theta = 42.5^\circ$ in the $[10\bar{1}0]$ plane, and at $\theta = 43.5^\circ$ in the $[11\bar{2}0]$ plane, at which angles the plane containing the orbits enclosing extremal area becomes tangent to the surface of the undulating cylinder.⁸ When θ is larger than the critical cutoff angles, the trajectories centered near H extend up and over the horizontal "ears" of the undulating cylinder and have a projection along the KH line greater than the height of the Brillouin zone. β_2 is the two-zone branch of this trajectory. It arises within $\frac{1}{2}^\circ$ of the angle where β_1 is cut off in the $[11\bar{2}0]$ plane. It should be noted that symmetry conditions require that the two-zone trajectories in this plane have an extremal area but that there are no such conditions on the two-zone trajectories for magnetic field directions in the $[10\bar{1}0]$ plane. Thus, it is not surprising that an equivalent branch of β_2 was not observed in the $[10\bar{1}0]$ plane.

γ is assigned to the extremal orbits about the belly of the undulating cylinder. The size and angular variation of γ require that the undulating cylinder make contact at the Brillouin-zone edge along the entire length of the KH line. γ is sharply cut off at $\theta = 68.5^\circ$ in the $[10\bar{1}0]$ plane and at $\theta = 73.5^\circ$ in the $[11\bar{2}0]$ plane, at which angles the plane containing the orbits enclosing extremal area becomes tangent to the surface of the undulating cylinder. γ_1 branches off from γ at $\theta = 22^\circ$ in the $[11\bar{2}0]$ plane and is cut off at $\theta \approx 55^\circ$. This branching results from the fact that the crevice between two adjacent "ears" of the undulating cylinder is quite deep, and symmetry demands that an extremal orbit be tied in the bottom of this crevice near K with an orbit axis along the KM zone line when the magnetic field is tilted in the $[11\bar{2}0]$ plane. For $\theta > 22^\circ$ the trajectories which pass near the tip of one of the ears enclose greater area than the trajectories locked in the crevice. Thus the area measured by γ changes from being a maximum external cross section to being a minimum extremal cross section at $\theta = 22^\circ$. Examples of the trajectories associated with γ and γ_1 are sketched on Fig. 2(b) for $\theta \approx 45^\circ$.

γ' has not been observed for magnetic field strengths below 32 kG. γ' branches off from γ at $\theta \approx 71^\circ$ as a result of magnetic breakdown across the spin-orbit-induced gap in the *AHL* plane between the "cap" in the first zone and the undulating cylinder in the second zone. The combination branch $\gamma\gamma'$ measures the extremal area of the closed surface obtained by magnetic breakdown. This surface is shown in Fig. 2(c). The combination branch $\gamma\gamma'$ is extremal at $(10\bar{1}0)$ and varies continuously from $(10\bar{1}0)$ to both (0001) and $(11\bar{2}0)$. These facts explicitly prove that the undulating cylinder makes contact with the zone edge along the entire length of the *KH* line.

We will now consider further information that the effects of magnetic breakdown have given about the nature of the undulating cylinder near *K*. Recalling the discussion of Bennett and Falicov,⁹ we note that the two energy bands of lowest energy in cadmium at *K* are doubly degenerate K_5 . Spin-orbit interactions split K_5 into two levels having K_8 and K_9 representations. Of these, K_9 lies lowest in energy, separated from K_8 by about 10^{-2} Ry. Our previous discussion showed that the cap terminated very near *K* and that the undulating cylinder enclosed *K*. Thus, we can assign K_9 to the cap and K_8 to the undulating cylinder with the Fermi level placed somewhere above K_9 but below K_8 . The pertinent point is that the gap separating K_8 and K_9 is sufficiently small that magnetic breakdown between the two sheets of the Fermi surface associated with these levels will be significant in fields of about 25 kG for magnetic field directions near (0001) . We have observed the effect of this breakdown. Figs. 3(a), 3(b), 3(c), and 3(d) show the types of trajectories which occur on the undulating cylinder in the ΓKM plane when magnetic breakdown occurs. In low fields the trifoliate trajectory shown in Fig. 3(a) applies. In very high fields the self-intersecting trifoliate trajectory shown in Fig. 3(d) is dominant. The areas enclosed by these two are essentially identical. At intermediate fields we also see the single-leaf and double-leaf trajectories shown in Figs. 3(b) and 3(c), respectively. The pertinent experimental area branches which we observed for magnetic fields along (0001) are $\gamma = 0.579 \text{ \AA}^{-2}$ which we identify with the trajectories in Figs. 3(a) and 3(d), $\gamma_{1/3} = 0.193 \text{ \AA}^{-2}$ associated with Fig. 3(b), and $\gamma_{2/3} = 0.386 \text{ \AA}^{-2}$ associated with Fig. 3(c).¹⁰

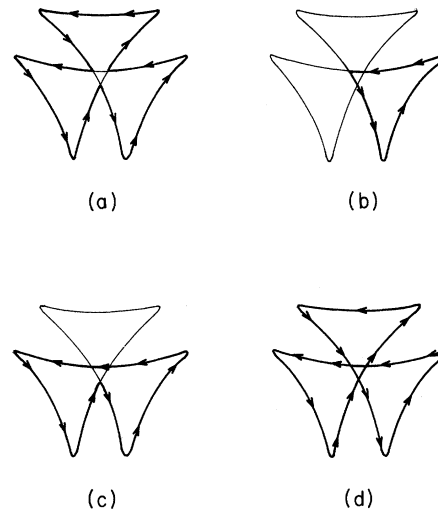


FIG. 3. The cross section of the undulating cylinder in the ΓKM plane of the Brillouin zone showing the types of trajectories that result from magnetic breakdown between the first and second zones near *K*. The small triangular section in the center is greatly exaggerated in size and is the cross section of the "free-electron" cap. The actual cap does not quite extend to *K* due to the presence of a very small band gap near *K* so that this piece of the surface must be considered to be virtual.

Both of the trajectories shown in Figs. 3(b) and 3(c) require two points of tunneling and one point of Bragg reflection. However, the Bragg reflection required to obtain the trajectory in Fig. 3(b) occurs on what must be considered a virtual piece of the Fermi surface. That is, it occurs on the "free-electron" cap in a region that is classically not contained in the cap since the cap does not quite extend to *K*. As a result the Bragg reflection occurring in this region is associated with the decaying tail of the wave function. Hence, the amplitude of the wave functions defining the trajectory in Fig. 3(b) will be considerably less than the amplitude of the wave function defining the trajectory in Fig. 3(c). This unusual amplitude difference was observed experimentally for the dHvA oscillations associated with $\gamma_{1/3}$ and $\gamma_{2/3}$.

Finally, we should note that magnetic breakdown near *K* in the Brillouin zone has previously been observed in beryllium, magnesium, and zinc where the breakdown occurred between the second and third zone sheets of the Fermi surface in contrast with cadmium where the

breakdown occurs between the first- and second-zone sheets of the Fermi surface.

We would like to express our appreciation to Professor L. M. Falicov for many interesting and stimulating discussions.

*Work supported in part by the Army Research Office (Durham), the Alfred P. Sloan Foundation, and the Advanced Research Projects Agency.

†ARO Research Assistant.

‡Alfred P. Sloan Research Fellow.

¹W. A. Harrison, Phys. Rev. **118**, 1190 (1960).

²M. H. Cohen and L. M. Falicov, Phys. Rev. Letters **5**, 544 (1960); and L. M. Falicov and M. H. Cohen, Phys. Rev. **130**, 92 (1963).

³See, for example, T. G. Berlincourt, Phys. Rev. **94**, 1172 (1954); A. S. Joseph, W. L. Gordon, J. R. Reitz, and T. G. Eck, Phys. Rev. Letters **7**, 334 (1961); J. K. Galt, F. R. Merritt, and P. H. Schmidt, Phys. Rev. Letters **6**, 458 (1961); J. D. Gavenda and B. C. Deaton, Phys. Rev. Letters **8**, 208 (1962); D. F. Gibbons and L. M. Falicov, Phil. Mag. **8**, 177 (1963); A. D. C. Grassie, Phil. Mag. **9**, 847 (1964).

⁴M. H. Cohen and L. M. Falicov, Phys. Rev. Letters

7, 231 (1961); E. I. Blount, Phys. Rev. **126**, 1636 (1962); A. B. Pippard, Proc. Roy. Soc. (London) **A270**, 1 (1962).

⁵R. W. Stark and L. R. Windmiller, to be published.

⁶The Onsager relation between the extremal cross-sectional area, \mathcal{Q} , (in \AA^{-2}) and the de Haas-van Alphen frequency, F (in gauss), is given by

$$\mathcal{Q} = (4\pi^2 e / ch) F = 9.55 \times 10^{-9} \times F.$$

⁷D. Shoenberg and P. J. Stiles, Proc. Roy. Soc. (London) **A281**, 62 (1964).

⁸I. M. Lifshitz and M. I. Kaganov, Usp. Fiz. Nauk. **69**, 419 (1959) [translation: Soviet Phys.—Usp. **2**, 831 (1960)].

⁹A. J. Bennett and L. M. Falicov, Phys. Rev. **136**, A998 (1964).

¹⁰J. K. Galt, F. R. Merritt, and J. R. Klauder, Phys. Rev. **139**, A823 (1965), associated two of the effective-mass branches which were observed in their cyclotron-resonance experiment in cadmium with orbits generated by this type of magnetic breakdown. However, neither their mass values measured along (0001) nor the angular variation of these mass branches agree with the values obtained in this experiment and must presumably be associated with some other trajectories on the Fermi surface.

PERMANENT PHOTOINDUCED CONDUCTIVITY IN SILVER HALIDE CRYSTALS

L. Cordone and M. U. Palma*

Istituto di Fisica dell'Università di Palermo, Palermo, Italy, and Gruppo di Palermo del Gruppo Nazionale Struttura della Materia del Consiglio Nazionale delle Ricerche, Palermo, Italy

(Received 25 October 1965)

In this Letter we report preliminary results which, in agreement with Mitchell's theory of photographic processes, show that it is possible to build up in a controllable way a finite and permanent concentration of electrons in the conduction band of silver halide crystals at low temperatures.

In order to have photoelectrons available to take part in the primary photographic process, a photoelectron-hole recombination must be avoided.¹ As Mitchell has emphasized, this can be obtained if (i) there exist in the crystal suitable traps for holes and (ii) following the hole capture, the same centers do not act as traps for electrons (otherwise they would simply act as recombination centers).

It follows immediately that if there exist conditions under which the two above requirements are satisfied and if furthermore the electrons are not allowed to take part in the primary photographic process, it may be possible in

principle to build up a permanent concentration of mobile electrons in the conduction band of silver halide crystals.

Previous work at this Laboratory²⁻⁵ has led us to investigate the role of positive-ion vacancies in the trapping of photoliberated holes. In order to control the number of vacancies in AgBr, we have used a doping with Cd⁺⁺ ions. Preliminary experiments showed remarkable electric losses at 10 Gc/sec in these crystals, as a result of illumination in the region of fundamental absorption and quick freezing at 77°K. These losses were permanent at 77°K; however, they annealed out by increasing the temperature above certain values.

To ascertain the nature of these losses, we have performed more extensive experiments at different frequencies. The main features of our results on AgBr: Cd⁺⁺ single crystals are the following:

(1) When the temperature is raised, the photo-